



# Seismic Performance Evaluation of Cold-Formed Steel Shear Walls Using Corrugated Steel Sheathing

Wenyong Zhang, S.M.ASCE<sup>1</sup>; Mahsa Mahdavian, S.M.ASCE<sup>2</sup>; Yuanqi Li, M.ASCE<sup>3</sup>; and Cheng Yu, M.ASCE<sup>4</sup>

**Abstract:** Cold-formed steel shear wall with corrugated sheet steel sheathing is a newly proposed lateral force resisting system from recent research work. The advantages of noncombustibility, high shear strength and high shear stiffness enable this new wall system to be a feasible solution for low- and midrise construction at high wind and seismic zones. The design provisions for this new type of shear wall have not been developed in current design specifications. The initial phase of this research project involved the displacement-based testing of bearing wall and shear wall specimens under combined lateral and gravity loading. The phase two research, presented here, includes the nonlinear finite element analysis and the performance evaluation of a set of light framed steel buildings using the corrugated sheet sheathed shear walls. Incremental dynamic analyses were performed on six archetype buildings and seismic performance assessment was evaluated. The results verify a set of seismic performance factors ( $R = C_d = 6.5$  and  $\Omega = 3.0$ ) for the corrugated sheet sheathed shear wall systems. **DOI:** 10.1061/(ASCE)ST.1943-541X.0001891. © 2017 American Society of Civil Engineers.

**Author keywords:** Corrugated sheet steel sheathing; Numerical simulation; Seismic performance assessment; Seismic performance modification factors; Metal and composite structures.

## Introduction

Cold-formed steel (CFS) shear wall using corrugated sheet steel sheathing is a newly proposed lateral resisting system from recent research (Fülöp and Dubina 2004; Stojadinovic and Tipping 2009; Yu et al. 2009; Yu 2013). CFS framed shear walls using corrugated steel sheathing have been found to yield higher strength, greater initial stiffness with similar ductility under cyclic loading when compared with the CFS walls using conventional sheathing materials.

However, the existing building codes and specifications—International Building Code (IBC 2012), Minimum Design Loads and Associated Criteria for Buildings and Other Structures [ASCE 7 (ASCE 2016)], AISI S240 North American Standard for Cold-Formed Steel Structural Framing, AISI S400 North American Standard for Seismic Design of Cold-Formed Steel Structural Systems—do not specify seismic performance factors for buildings using the CFS corrugated steel sheathing shear walls. Systematic investigation is needed to support this newly proposed lateral force resistance system to be used in actual buildings. The initial phase of the research effort comprised the monotonic and cyclic tests of full-scale CFS framed bearing walls and shear walls using corrugated steel sheathing under combined lateral and gravity loading. Zhang et al. (2016) reports the details of Phase I work. The major objectives of the Phase I tests were to obtain the collapse drift limit and to investigate the seismic performance of this new wall system.

Presented in the paper is the phase two of this research project, which includes the numerical simulation of typical low- and mid-rise light-framed CFS buildings using corrugated sheet sheathed shear walls as the primary lateral force resisting system. FEMA P695 (FEMA 2009) methodology was adopted, and a number of six building archetypes were simulated in a finite element software *OpenSees*. The paper gives a brief description of the test results and detailed modeling information and the relevant seismic performance assessment.

## Experimental Results

Displacement-control based testing of wall specimens with corrugated sheet steel sheathings were completed at the University of North Texas (Zhang et al. 2016). A total of eight full-scale wall specimens were tested under a combined lateral and vertical/gravity loading condition. The test program included four shear walls and four bearing walls. The framing members used Steel Studs Manufacturers Association (SSMA) structural stud 350S200-68 (345 MPa) and track 350T150-68 (345 MPa). The sheathing consisted of three Shallow Verco Decking SV36 corrugated steel sheets with 0.686 mm (27 mil) thickness and 14.3 mm (9/16 in.) rib height. The shear wall specimens used double C-shaped sections for the chord/boundary studs and one C-shaped section as the vertical field stud. Two hold-downs and two shear bolts were used to secure the shear wall specimens to the test bed. The bearing wall specimens used one single stud for the middle and chord stud. No hold-down was placed for bearing walls following engineering practices. Four shear bolts were used to anchor the bottom track to the test bed. Fig. 1 shows the details of the two wall configurations.

The procedure of the monotonic tests was in accordance with ASTM E564 (ASTM 2012a) “Standard Practice for Static Load Test for Shear Resistance of Framed Walls for Buildings.” The cyclic tests followed the method C in ASTM E2126 (ASTM 2012b) “Standard Test Methods for Cyclic (Reversed) Load Test for Shear Resistance of Vertical Elements of the Lateral Force Resisting Systems for Buildings.” The load versus displacement

<sup>1</sup>Ph.D. Candidate, Dept. of Structural Engineering, Tongji Univ., Shanghai 200092, China. E-mail: wenyongzhang@163.com

<sup>2</sup>Graduate Student, Dept. of Engineering Technology, Univ. of North Texas, Denton, TX 76207. E-mail: mahsa\_mahdavian@yahoo.com

<sup>3</sup>Professor, Dept. of Structural Engineering, Tongji Univ., Shanghai 200092, China. E-mail: liyq@tongji.edu.cn

<sup>4</sup>Professor, Dept. of Engineering Technology, Univ. of North Texas, Denton, TX 76207 (corresponding author). E-mail: cheng.yu@unt.edu

Note. This manuscript was submitted on December 12, 2016; approved on May 12, 2017; published online on August 29, 2017. Discussion period open until January 29, 2018; separate discussions must be submitted for individual papers. This paper is part of the *Journal of Structural Engineering*, © ASCE, ISSN 0733-9445.

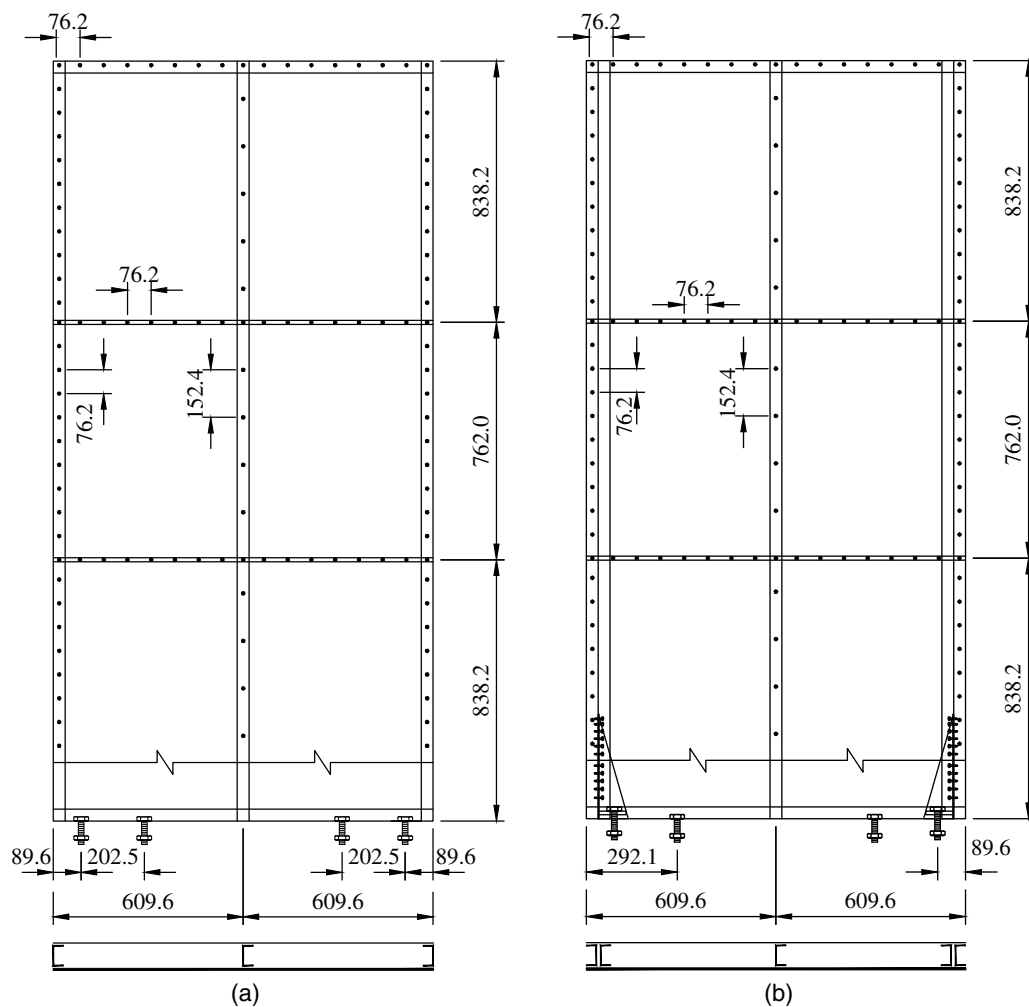


Fig. 1. Wall configurations: (a) bearing wall specimen; (b) shear wall specimen

curve of the corrugated sheet sheathed wall specimens under monotonic lateral loading and the typical hysteresis curve under cyclic lateral loading are illustrated in Fig. 2. In all tests, a constant vertical load of 24 kN was applied to the top track of the wall. The observed failure modes of the bearing wall were edge tearing of bottom sheathing and shear failure of framing screws at the wall corners. The observed failure modes of the shear wall were shear buckling of the corrugated sheet and screw pulling over of the bottom sheathing. Table 1 lists the average results of each wall configuration in the previous test program. The bearing walls contribute 34% of the shear strength and 35% of the dissipated energy in comparison with shear walls. As a result, the inclusion of bearing walls would be necessary in the numerical simulations of the building system analysis to appropriately reflect the actual behavior of CFS buildings. The monotonic tests also revealed that the bearing walls could reach the maximum drift of 6.8% without collapse (no reduction in gravity load capacity). For the shear walls, a maximum drift of 10.0% without collapse was observed in the tests.

### Building Archetypes

A building archetype is a prototypical representation of a seismic-force-resisting system. Archetypes are intended to reflect the wide range of design parameters and building attributes. The archetype can be assembled into performance groups based on their major

differences in plan configuration, building height, building occupancy, design gravity, and seismic load intensity. A total of six building archetypes differing in location (seismic intensity), occupancy type, and building height (number of stories) were selected in this study, as listed in Table 2. The following assumptions are made in the archetype definition:

1. Building occupancy: two baseline structures are considered in this study. The two baseline structures differ in the plan layout, the building size, and the applied live load intensity. The first one is a typical hotel building, with plan dimensions of  $20.30 \times 15.19$  m. The shear walls are located at the corners and two longitudinal sides. The bearing walls are placed primarily in the interior of the building. The second one is an office building similar to an archetype used in the NEES-CFS project (Madsen et al. 2011) which adopts an open-space concept design. All shear walls and bearing walls are placed along the exterior skin, and the overall plan dimensions are  $15.2 \times 7$  m. Fig. 3 shows the plan layouts of these two building archetypes.
2. Number of stories: two–five. Note that according to Table 504.4 in the current IBC (2012), building constructed with noncombustible material can increase the building height from three to five stories. As a result, the maximum of five stories is considered in this research.
3. Seismic design category (SDC): the archetypes are designed for SDC D per ASCE 7-16 (ASCE 2016). The maximum considered earthquake (MCE) spectral response acceleration

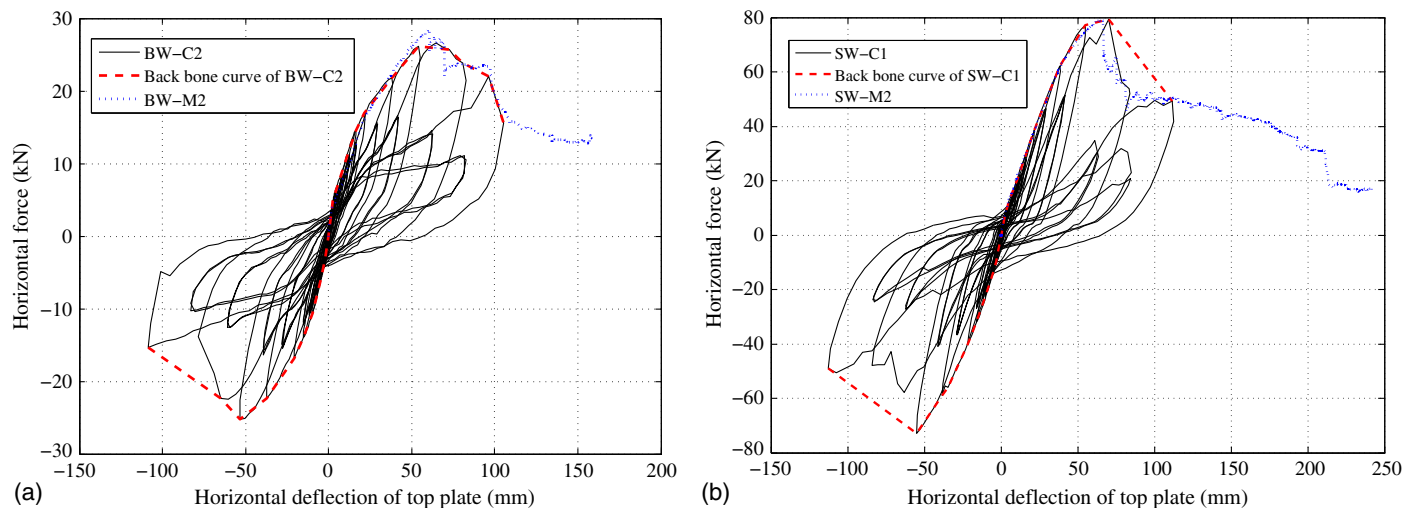


Fig. 2. Test results: (a) bearing wall results; (b) shear wall results

Table 1. Summary of Test Results

Label	Aspect ratio	Loading protocol	Ultimate strength (kN/m)	$\Delta$ (mm)	Ductility factor	Energy (J)
BW	4 × 8	M	25.1	60.5	2.23	1,438
	4 × 8	C	20.1	59.4	4.27	1,637
SW	4 × 8	M	68.5	66.6	1.96	3,880
	4 × 8	C	62.4	62.7	2.61	4,968

Note: BW = bearing wall; C = cyclic; M = monotonic; SW = shear wall.

Table 2. Archetype Buildings

Archetype identifier	Number of stories	Occupancy	Key archetype design parameters			
			Aspect ratio	$S_{MT}$ (g)	T (s)	V/W (g)
1	2	Hotel	2	1.5	0.262	0.154
2	4	Hotel	2	1.5	0.440	0.154
3	5	Hotel	2	1.5	0.520	0.154
4	2	Office	2.72	1.39	0.245	0.143
5	3	Office	2.72	1.39	0.332	0.143
6	5	Office	2.72	1.39	0.486	0.143

Note:  $S_{MT}$  = maximum considered earthquake spectral acceleration; T = fundamental period calculated according to Section 5.2.5 in FEMA P695 (FEMA 2009).

parameter for short-period  $S_{mt} = 1.5g$  is used for the first baseline structure—hotel building and  $S_{mt} = 1.39g$  for the second baseline structure—office building.

- Design criteria: The load resistance factor design (LRFD) design method was applied, and the seismic force modification factors were initially set based on the light-frame steel shear resistance systems with flat steel sheathing [ASCE 7-16 (ASCE 2016)].  $R = 6.5$  and  $\Omega = 3.0$  were used in the building design, subjected to confirmation by this study.

## Numerical Modeling

The building archetypes were designed according to ASCE 7-16 (ASCE 2016). Seismic lateral force resistance was assumed to

be provided by the shear walls. The total story shear was first determined, and the length and distribution of the shear wall were then assigned. The shear wall resistance was based on the test results by Zhang et al. (2016), and a resistance factor of  $\varphi = 0.6$  was used following the provisions in AISI S400 (AISI 2015).

The nonlinear dynamic analysis software *OpenSees* (McKenna et al. 2010) was used in the finite element (FE) analysis. Fig. 4 illustrates the schematic drawings of the two-story FE models used in *OpenSees*. As discussed before, the simulation of the bearing wall was also included in the building model. The bearing walls of the office building were primarily along the exterior skin, which allowed the flexible arrangement of the partition walls. For the hotel building, the bearing walls were primarily the interior walls, which allowed the existence of large window openings on the exterior walls. It is noted that such an arrangement is appropriate and conservative for the FE modeling.

## Modeling of Shear Walls

The shear walls were simulated in *OpenSees* as two diagonal truss elements and elastic frame boundary elements as illustrated in Fig. 5. The rigid connection method was used because the linear static analysis results showed that the diagonal bracing stiffness greatly exceeded the small moment stiffness of the stud-to-track connection. To achieve the pinching effect, the strength degradation and the stiffness degradation of the shear wall, the Pinching4 uniaxial hysteretic material in *OpenSees* were used for the diagonal truss elements. To obtain the backbone curve of the Pinching4 material, the horizontal load (V) versus deflection ( $\Delta$ ) was first converted to a stress-strain relationship:

The axial force in the diagonal bracing F can be expressed as:

$$F = V / (2 \cos \theta)$$

The stress and strain in the diagonal bracing can be obtained as:

$$\sigma = F / A = V / (2A \cos \theta)$$

$$\varepsilon = d / l = (\Delta \cos \theta) / l$$

where  $\cos \theta = b / \sqrt{b^2 + h^2}$ ,  $l = \sqrt{b^2 + h^2}$ ;  $b$ ,  $h$  = width and height of the shear wall, respectively.

The backbone curve and pinching parameters (reloading and unloading) of shear walls were based on the Phase 1 test results

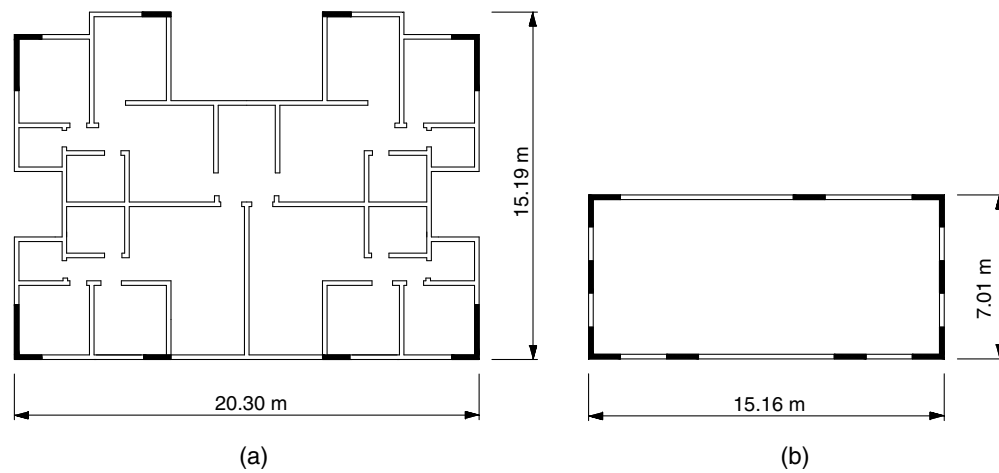


Fig. 3. Plan layouts: (a) hotel building; (b) office building

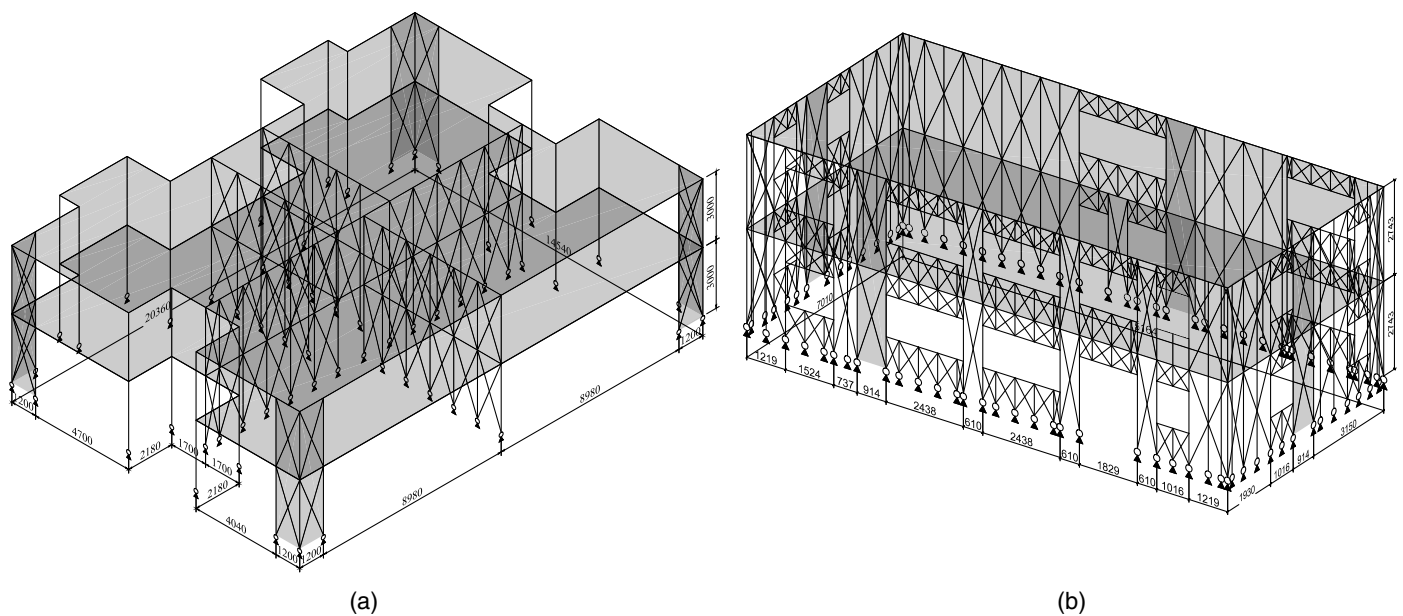


Fig. 4. *OpenSees* models: (a) two-story hotel building; (b) two-story office building

reported in Zhang et al. (2016). The aspect ratio adjustment recommended in AISI S400 (AISI 2015) was performed when the width of the wall in the building was different from the width of test specimen. A comparison example of the *OpenSees* result with the test result is illustrated in Fig. 6, in which the comparisons of the last 15 cyclic loops are also provided. The shear wall model has a good agreement with the test result, and the model was able to simulate the postpeak behavior of the shear wall.

### Modeling of Bearing Walls

In the building model, the bearing walls were designed to have the same sheathing material as the shear walls. Shear resistance of the bearing walls was considered in the FE analysis. The modeling technique of bearing walls was the same as the shear walls. The backbone curve and the pinching perimeters (reloading and unloading) of the bearing walls were based on the Phase 1 test results reported in Zhang et al. (2016).

As for the small bearing walls at the opening locations (windows and doors), a detailed FE model using *ABAQUS* was created.

The *ABAQUS* modeling techniques were reported in Mahdavian et al. (2016). All framing members and the corrugated sheet sheathings were modeled with S4R shell elements. The connections between the framing members used tie constraints, and the connections between the sheathing and the framing members used nonlinear Spring2 elements. Each spring connection contained three spring elements, one withdrawal spring and two shear springs. Material properties were based on coupon test results. The bottom of the shear wall was restrained in all three directions, and two lines of nodes on the web of the top track were restricted in the out-of-plane direction to simulate the lateral support. The vertical direction of all the nodes at the hold-down area of each chord stud was restrained. Surface-to-surface contact was introduced between the frame and the corrugated sheets to prevent the sheathing from penetrating the frame members. Contact properties of frictionless tangent behavior and hard-contact normal behavior were used. All the nodes on the web of the top track were coupled to a reference point located on the edge of the top track. A displacement controlled lateral load was applied to the reference point in the horizontal direction. In *ABAQUS*, the observed failure was the buckling of the

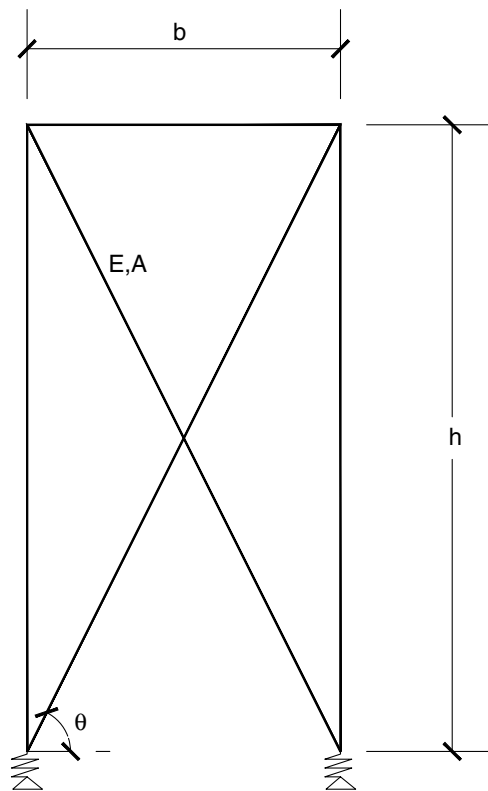


Fig. 5. Shear wall modeling

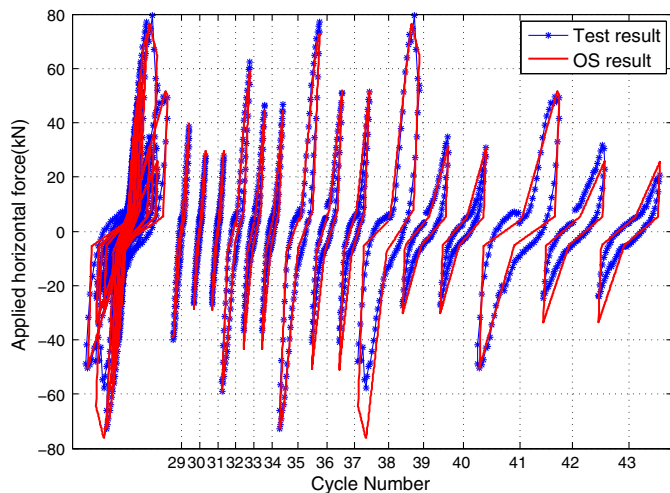


Fig. 6. Simulation results of shear wall

corrugated sheet and a slight torsional and local buckling of the chord studs, which was inconsistent with the test results. A comparison of the load-deformation responses is illustrated in Fig. 7, which indicates that the *ABAQUS* model has a good agreement with the test result. The load versus displacement curve from the FE analyses was then used as the backbone curve for the small bearing walls. The pinching parameters (reloading and unloading) remained the same as the test data in Zhang et al. (2016).

### Modeling of Diaphragms

A rigid diaphragm was used in the building model by a built-in element in *OpenSees*. The rigid diaphragm element required a

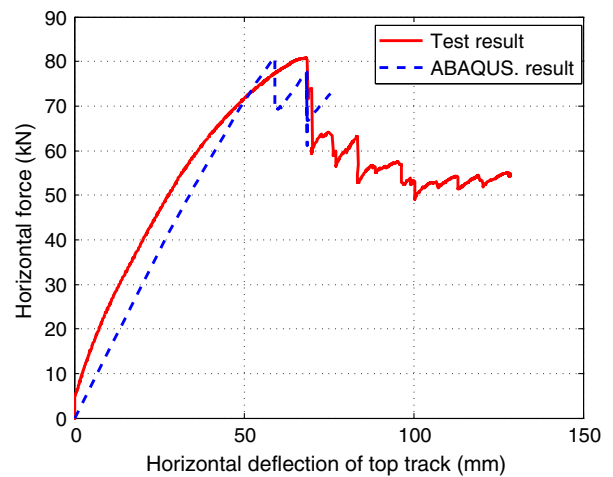


Fig. 7. Load versus displacement responses

master-slave relationship of nodes in the same plane. Lateral displacement in two directions and rotation about the vertical axis were defined at the master node.

### Seismic Mass and Gravity Load

Total seismic mass was calculated according to ASCE 7-16 (ASCE 2016), and the mass of each story was divided equally and lumped to the four corners. Gravity load of the building should be added separately because seismic mass is only related to the mass matrix in the FE formulation. The weight applied here was the product of the seismic mass and the acceleration of gravity ( $g$ ). The P-delta effect was included because large displacement might arise.

### Nonlinear Static (Pushover) Analysis

The objective of nonlinear static (pushover) analysis was to obtain the ductility parameter and over-strength factor of the building system. The applied lateral force at each story level was in proportion to the fundamental mode shape of the index archetype model. The displacement ductility factor is defined as  $\mu_T = \delta_u / \delta_y$ , where  $\delta_u$  = ultimate displacement and  $\delta_y$  = displacement at yield. FEMA P695 (FEMA 2009) defines  $\delta_u$  as the roof displacement at the point of 20% strength loss ( $0.8V_{max}$ ). The over-strength factor is defined as  $\Omega_0 = V_{max} / V_{design}$ , where  $V_{max}$  = maximum base shear in actual behavior and  $V_{design}$  = base shear at design level. The displacement ductility factor and over-strength factor of the six building archetypes are listed in Table 3. Typical pushover curves of the building archetypes are shown in Fig. 8.

### Incremental Dynamic Analysis

Nonlinear time history analysis lies in the core of the incremental dynamic analysis (IDA) method, where the structure is subjected to a suite of ground motion records. Each record is scaled to multiple levels of intensity until a designated damage measure (DM) limit for collapse is reached. IDA produces the structure's capacity curve in terms of structure DM versus an intensity measure (IM). Story drift is a typical DM, and the spectral acceleration of the first natural period of the structure is a typical IM.

To avoid bias, a specified set of ground motion records should be utilized as excitations. FEMA P695 (FEMA 2009) recommends two sets of ground motion records for collapse assessment using

**Table 3.** Pushover Results

Occupancy	Height	$\Omega_0$	$\mu_T$
Office building	2-story	8.69	2.07
	3-story	6.17	1.74
	5-story	3.84	1.92
	Mean	6.23	1.91
Hotel building	2-story	4.93	1.95
	4-story	3.03	1.64
	5-story	2.87	1.83
	Mean	3.61	1.80

nonlinear dynamic analysis: Far-field record and near-field record set. The far-field record set includes 22 component pairs of horizontal ground motions from sites located greater than or equal to 10 km from fault rupture. The record sets do not include the vertical component of ground motion because this direction of earthquake shaking is not considered of primary importance for collapse evaluation, and is not required by the FEMA P695 Methodology for nonlinear dynamic analysis. The near-field record set is only for supplemental information and is used in special studies to evaluate potential differences in the collapse margin ratio (CMR) for SDC E structures. As a result, the far-field record set was chosen, and horizontal components of ground motion were used.

The median collapse intensity,  $S_{CT}$ , is defined as the spectral acceleration causing 50% collapse probability. The ratio between

the median collapse intensity ( $S_{CT}$ ) and the MCE intensity ( $S_{MT}$ ) is the CMR. CMR is the primary parameter used to evaluate the collapse safety of the building design. The Phase 1 tests showed that the corrugated steel sheathing shear wall could reach 10% drift without collapse. FEMA P695 (FEMA 2009) adopted 7% as the collapse drift limit for the light-framed wood shear wall system. Because the building codes [IBC 2012; ASCE7 (ASCE 2016)] consider the light framed wood and steel shear wall systems to have the same seismic performance, the authors conservatively chose 7% as the drift limit for the CFS corrugated steel sheathing shear wall system in IDA. Typical IDA curves and fragility curves of the building archetypes are shown in Figs. 9 and 10, respectively.

## Seismic Performance Evaluation

The concepts of the seismic performance factors can be illustrated with Fig. 11. The term of a response modification factor is based on the argument that well-designed structural resistant systems have a ductile behavior and are able to carry large inelastic deformation without collapse. As a result, the designed seismic strengths given by earthquake-resistant design codes are typically lower than the lateral strength that is required to keep a structure in the elastic range in the event of earthquakes. This reduction in the design strengths is represented using the response modification factor  $R$ :

$$R = V_E/V_{\text{design}}$$

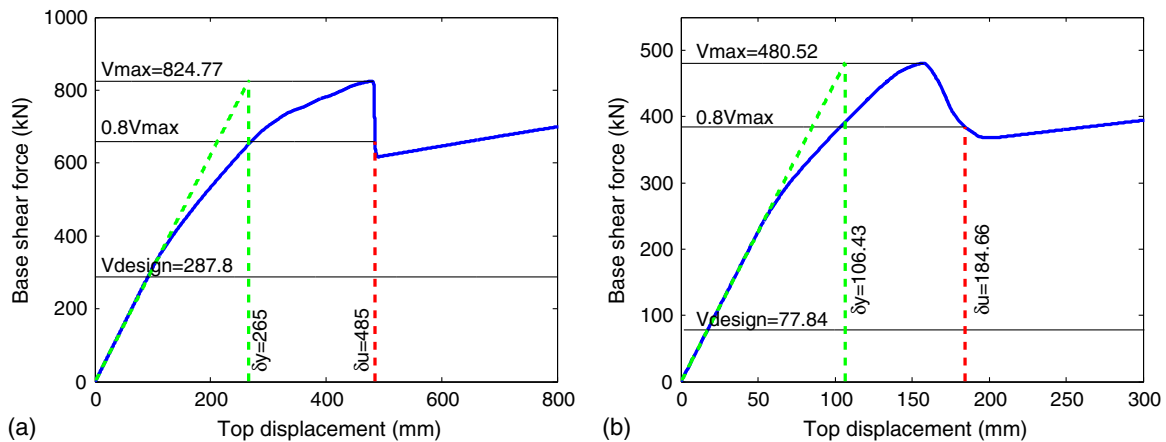


**Fig. 8.** Pushover curves: (a) five-story hotel building; (b) three-story office building

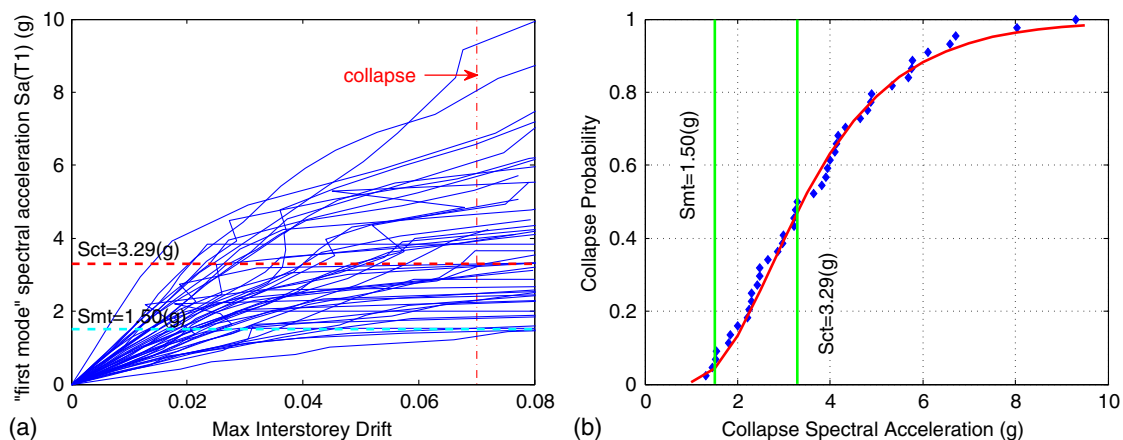


**Fig. 9.** IDA results of five-story hotel building: (a) IDA curve; (b) fragility curve

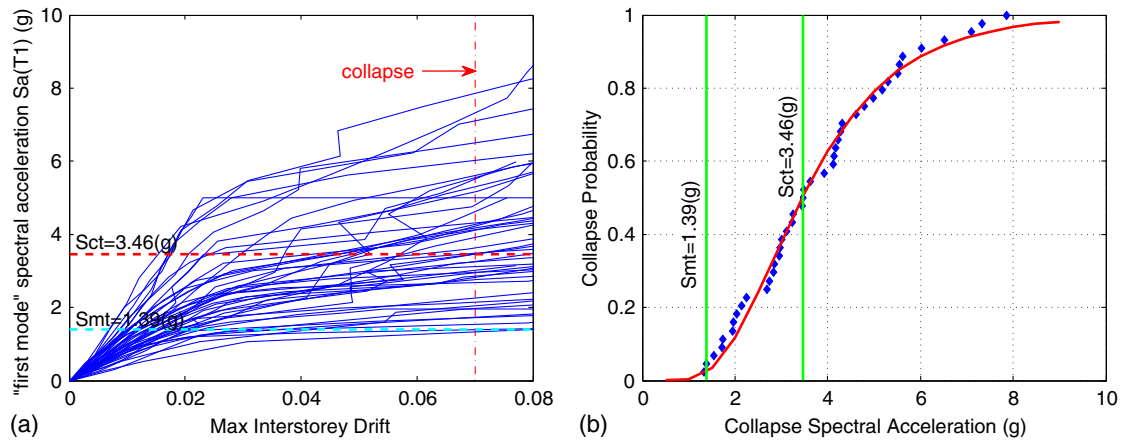


Fig. 10. IDA results of three-story office building: (a) IDA curve; (b) fragility curve

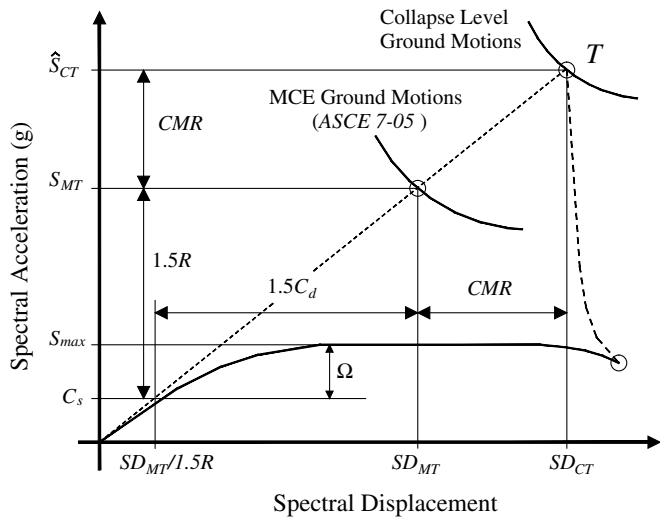


Fig. 11. Illustration of seismic performance factors ( $R$ ,  $\Omega$ , and  $C_d$ ) (reprinted from FEMA P695 2009)

where  $V_E$  = shear force that would be developed in the seismic-force-resisting system if the system remained entirely linearly elastic for design earthquake ground motions;  $V_{design}$  = base shear at design level.

The over-strength factor is intended to address possible sources that may contribute to strength beyond its nominal value, such as structural redundancy, use of strength reduction factors and load factors in design, use of multiple loading combinations, nonstructural elements effects. The over-strength factor can be expressed as:

$$\Omega_0 = V_{max}/V_{design}$$

where  $V_{max}$  = maximum base shear in actual behavior.

Seismic design provisions estimate the maximum roof and story drifts occurring in major earthquakes by amplifying the drifts computed from elastic analysis at the prescribed design seismic force level with a deflection amplification factor ( $C_d$ ). Recommended values of these three seismic performance factors will be discussed hereinafter.

### Calculation of Over-Strength Factor $\Omega_0$

This section determines the value of the over-strength factor,  $\Omega_0$ , which would be used in the design provisions for this newly

proposed lateral resisting system. Table 3 summarizes the calculated  $\Omega$  values for each archetype, with a range of values from 2.87 to 8.69. The average values for each performance group are 6.23 and 3.61, with the largest value of 6.23. According to FEMA P695 (FEMA 2009), the largest possible  $\Omega_0 = 3.0$  is warranted, with the average values being greater than 3.0 for both of the performance groups.

### Calculation of Response Modification Factor $R$

The collapse capacity of building structures can be influenced by different sources of uncertainty. The sources of uncertainty include: uncertainty attributable to record-to-record variation,  $\beta_{RTR}$ ; uncertainty owing to design requirements,  $\beta_{DR}$ ; uncertainty related to the test data,  $\beta_{TD}$ ; and uncertainty related to modeling of the structure,  $\beta_{MDL}$ . FEMA P695 (FEMA 2009) quantifies each of these uncertainties based on the following scale: (1) superior,  $\beta = 0.10$ ; (2) good,  $\beta = 0.20$ ; (3) fair,  $\beta = 0.35$ ; and (4) poor,  $\beta = 0.50$ . The total system collapse uncertainty,  $\beta_{TOT}$ , is calculated based on these four uncertainties:  $\beta_{TOT} = \sqrt{\beta_{RTR}^2 + \beta_{DR}^2 + \beta_{TD}^2 + \beta_{MDL}^2}$ . To account for the effects of the frequency content (spectral shape) of the applied earthquake record set, the CMR was adjusted using the spectral shape factor (SSF). For each building archetype, the adjusted collapse margin ratio, ACMR, was calculated by multiplying the CMR by SSF.

Table 4 summarizes the aforementioned data, specifically, the median collapse intensity,  $S_{CT}$ , the collapse margin ratio, CMR, the adjusted collapse margin ratio, ACMR, and is compared with the reference value given in FEMA P695 (FEMA 2009). The record-to-record collapse uncertainty is calculated based on  $0.2 \leq \beta_{RTR} = 0.1 + 0.1\mu_T \leq 0.4 (\mu_T \leq 3)$ . The design requirements-related uncertainty, the test data related uncertainty, and modeling of structure related uncertainty were taken as good. To account for the impact of the selection of quality ratings, a comparison is provided in Table 5, in which the design requirements-related uncertainty and the modeling of structure related uncertainty were taken as fair. The test data related uncertainty remained as good because previous experimental experience shows that as long as the boundary condition (test setup) remains the same, the test results should be reliable.

Results in Tables 4 and 5 show that the ACMR for each archetype well passes the acceptable collapse margin ratio with 20% collapse probability (ACMR 20%), and the average value of ACMR for each performance group exceeded the acceptable collapse margin ratio with 10% collapse probability (ACMR 10%). As a result,

**Table 4.** IDA Results

Occupancy	Height	$S_{CT}$	CMR	SSF	ACMR	$\beta_{TOT}$	Accept ACMR
Office building	2-story	3.84	2.76	1.061	2.929	0.463	1.476
	3-story	3.46	2.49	1.049	2.611	0.441	1.449
	5-story	3.69	2.65	1.125	2.981	0.453	1.464
	Mean of performance group	3.66	2.633	1.078	2.840	0.452	1.785
Hotel building	2-story	3.20	2.13	1.058	2.256	0.455	1.466
	4-story	3.25	2.17	1.046	2.266	0.436	1.443
	5-story	3.29	2.20	1.055	2.136	0.447	1.456
	Mean of performance group	3.25	2.167	1.053	2.219	0.446	1.770

**Table 5.** IDA Results

Occupancy	Height	$S_{CT}$	CMR	SSF	ACMR	$\beta_{TOT}$	Accept ACMR
Office building	2-story	3.84	2.76	1.061	2.929	0.616	1.679
	3-story	3.46	2.49	1.049	2.611	0.600	1.660
	5-story	3.69	2.65	1.125	2.981	0.588	1.641
	Mean of performance group	3.66	2.633	1.078	2.840	0.601	2.163
Hotel building	2-story	3.20	2.13	1.058	2.256	0.610	1.672
	4-story	3.25	2.17	1.046	2.266	0.596	1.654
	5-story	3.29	2.20	1.055	2.136	0.604	1.665
	Mean of performance group	3.25	2.167	1.053	2.219	0.603	2.168

the adoption of  $R = 6.5$  are guaranteed for this newly proposed building system with corrugated sheet steel sheathing.

### Calculation of Deflection Amplification Factor $C_d$

The deflection amplification factor,  $C_d$ , is usually some fraction of the acceptable value of the response modification factor,  $R$ , related to the inherent damping of the system of interest. According to Eqs. (7) and (8) in FEMA P695 (FEMA 2009):

$$C_d = \frac{R}{B_I}$$

in which  $B_I$  is a numerical damping coefficient that can be obtained from Table 18.6.1 of ASCE 7 (ASCE 2016).

The inherent damping of the CFS framed building system with corrugated sheet steel sheathing was assumed to be 5% of the critical in this research. As a result, the damping coefficient,  $B_I$ , equals to 1.0, and the deflection amplification factor,  $C_d$ , equals to 6.5.

However, the inherent damping of the CFS framed building system with corrugated sheet steel sheathing still needs to be verified by future investigations. According to the test results by Schafer (2015), the measured damping of the CFS framed building using wood sheathed shear walls varied from 4 to 9%. Therefore, the adoption of 5% inherent damping in this research is believed to be conservative and appropriate.

### Conclusions

Numerical models of CFS framed buildings using corrugated steel sheathing in walls were created in the *OpenSees* program. Nonlinear FE analyses were performed on six building archetypes, and a seismic performance assessment was evaluated following the methodology in FEMA P695 (FEMA 2009). The results of the dynamic analysis indicate that a set of seismic performance factors ( $R = C_d = 6.5$  and  $\Omega = 3.0$ ) is appropriate for the new type of shear wall system. The proposed seismic performance factors are consistent with the existing factors for the CFS framed shear wall

systems using flat steel sheet or wood based panels. The proposed seismic performance factors shall also be evaluated and approved by professional experts before submitted to design documents. The paper serves as an analytical preparation for future code adoption of the new CFS shear wall system.

### Acknowledgments

This paper was prepared as part of the U.S. National Science Foundation grant, NSF-CMMI-0955189: Comprehensive Research on Cold-Formed Steel Sheathed Shear Walls, Special Detailing, Design, and Innovation. The research was also partially supported by the Chinese National Science Foundation Grant No. 51538002. Any opinions, findings, and conclusions or recommendations expressed in this article are those of the authors and do not necessarily reflect the views of the sponsors.

### References

- ABAQUS version 6.14 [Computer software]. Dassault Systèmes, Waltham, MA.
- AISI (American Iron and Steel Institute). (2015). "North American Standard for seismic design of cold-formed steel structural systems." *AISI S400*, Washington, DC.
- ASCE. (2016). "Minimum design loads for buildings and other structures." *ASCE 7*, Reston, VA.
- ASTM. (2012a). "Standard practice for static load test for shear resistance of framed walls for buildings." *ASTM E564*, West Conshohocken, PA.
- ASTM. (2012b). "Standard test methods for cyclic (reversed) load test for shear resistance of vertical elements of the lateral force resisting systems for buildings." *ASTM E2126*, West Conshohocken, PA.
- FEMA. (2009). "Qualifications of building seismic performance factors." *FEMA P695*, Washington, DC.
- Fülöp, L. A., and Dubina, D. (2004). "Performance of wall-stud cold-formed shear panels under monotonic and cyclic loading. I: Experimental research." *Thin Walled Struct.*, 42(2), 321–338.
- IBC (International Building Code). (2012). *International building code*, International Code Council, Washington, DC.

- Madsen, R. L., Nakata, N., and Schafer, B. W. (2011). "CFS-NEES building structural design narrative." ([www.ce.jhu.edu/cfsness](http://www.ce.jhu.edu/cfsness)) (May 15, 2015).
- Mahdavian, M., Zhang, W., Ding, C., Moen, C., and Yu, C. (2016). "Cyclic simulation of cold-formed steel shear walls with corrugated steel sheathing." *Proc., Annual Stability Conf.*, Structural Stability Research Council, Chicago.
- McKenna, F., Scott, M. H., and Fenves, G. L. (2010). "Nonlinear finite-element analysis software architecture using object composition." *J. Comput. Civil Eng.*, 10.1061/(ASCE)CP.1943-5487.0000002, 95–107. *OpenSees* [Computer software]. PEER, Berkeley, CA.
- Schafer, B. W. (2015). "Seismic response and engineering of cold-formed steel framed buildings." *Proc., 8th Int. Conf. on Advances in Steel Structures*, Univ. of Lisbon, Lisbon, Portugal.
- Stojadinovic, B., and Tipping, S. (2009). "Structural testing of corrugated sheet steel shear walls." *Technical Rep. to the Charles Pankow Research Foundation for Project No. CFC 03-06*, Univ. of California, Berkeley, CA.
- Yu, C., Huang, Z., and Vora, H. (2009). "Cold-formed steel framed shear wall assemblies with corrugated sheet steel sheathing." *Proc., Annual Stability Conf.*, Structural Stability Research Council, Phoenix.
- Yu, G. (2013). "Cold-formed steel framed shear wall sheathed with corrugated steel sheet." Masters thesis, Univ. of North Texas, Denton, TX.
- Zhang, W., Mahdavian, M., Li, Y., and Yu, C. (2016). "Experiments and simulations of cold-formed steel wall assemblies using corrugated steel sheathing subjected to shear and gravity loads." *J. Struct. Eng.*, 04016193.